NeuroImage 157 (2017) 521–530

Contents lists available at ScienceDirect

NeuroImage

journal homepage: www.elsevier.com/locate/neuroimage

Individual differences in functional connectivity during naturalistic viewing conditions

Tamara Vanderwal[a,*], Jeffrey Eilbott[a], Emily S. Finn[a], R. Cameron Craddock[b,c], Adam Turnbull[a], F. Xavier Castellanos[d]

[a] Yale University, 230 South Frontage Road, New Haven, CT 06520, USA
[b] Child Mind Institute, 445 Park Avenue, New York, NY 10022, USA
[c] Nathan Kline Institute for Psychiatric Research, 140 Old Orangeburg Road, Orangeburg, NY 10962, USA
[d] Child Study Center at New York University Langone Medical Center, 1 Park Avenue, New York, NY 10016, USA

ARTICLE INFO

Keywords:
Naturalistic viewing
fMRI
Identification algorithm
Inscapes
Movies

ABSTRACT

Naturalistic viewing paradigms such as movies have been shown to reduce participant head motion and improve arousal during fMRI scanning relative to task-free rest, and have been used to study both functional connectivity and stimulus-evoked BOLD-signal changes. These task-based hemodynamic changes are synchronized across subjects and involve large areas of the cortex, and it is unclear whether individual differences in functional connectivity are enhanced or diminished under such naturalistic conditions. This work first aims to characterize variability in BOLD-signal based functional connectivity (FC) across 2 distinct movie conditions and eyes-open rest (n=31 healthy adults, 2 scan sessions each). We found that movies have higher within- and between-subject correlations in cluster-wise FC relative to rest. The anatomical distribution of inter-individual variability was similar across conditions, with higher variability occurring at the lateral prefrontal lobes and temporoparietal junctions. Second, we used an unsupervised test-retest matching algorithm that identifies individual subjects from within a group based on FC patterns, quantifying the accuracy of the algorithm across the three conditions. The movies and resting state all enabled identification of individual subjects based on FC matrices, with accuracies between 61% and 100%. Overall, pairings involving movies outperformed rest, and the social, faster-paced movie attained 100% accuracy. When the parcellation resolution, scan duration, and number of edges used were increased, accuracies improved across conditions, and the pattern of movies > rest was preserved. These results suggest that using dynamic stimuli such as movies enhances the detection of FC patterns that are unique at the individual level.

1. Introduction

As psychiatric research has shifted towards a dimensional conceptualization of symptoms and behaviors (Insel et al., 2010), neuroimaging has expanded to include brain-based characterization at the individual level (Arbabshirani et al., 2013). Despite the reliability of BOLD-signal based functional connectivity (FC) patterns across individuals and testing sessions (Damoiseaux et al., 2006; O'Connor et al., 2016; Shehzad et al., 2009; Yeo and Krienen et al., 2011; Zuo et al., 2010), FC relationships have also been shown to capture significant inter-individual variability, generating optimism for their eventual use as biomarkers of mental illness (Finn and Shen et al., 2015; Gordon et al., 2017; Rosenberg et al., 2016; Shen et al., 2017). Recent work has begun to characterize the spatial and state-based aspects of individual differences in FC. The current study tests whether individually unique patterns of FC can be detected when the brain engages in the complex, dynamic processing that occurs when watching movies. We also examine multiple aspects of FC variability to better understand what factors might contribute to the detection of individually distinct FC patterns under naturalistic conditions.

1.1. Spatial distribution of FC variability

Functional neuroimaging data sets containing retest scans have been leveraged to investigate inter-individual variability in FC patterns, after regressing out intra-individual variability. Mueller et al. demonstrated that this residual variability in FC was greatest in association cortex including lateral prefrontal regions and the temporoparietal junction (Mueller et al., 2013). Unsurprisingly, unimodal sensory and motor regions were the least variable across subjects. At the network

* Corresponding author.
E-mail address: tamara.vanderwal@yale.edu (T. Vanderwal).

http://dx.doi.org/10.1016/j.neuroimage.2017.06.027
Received 4 April 2017; Received in revised form 9 June 2017; Accepted 13 June 2017
Available online 16 June 2017
1053-8119/

level, frontoparietal and ventral attention networks exhibited the largest variability in FC, followed next by the default and dorsal attention networks. This pattern of results was subsequently confirmed independently (Chen et al., 2015).

A second wave of studies extended these findings by using unsupervised test-retest sorting algorithms to match pairs of FC matrices that belong to a single subject from a group of FC matrices. Just as the Mueller approach above relied on the relationship between inter- and intra-subject variability, these matching algorithms require that a subject's intra-subject FC correlation be greater than that same subject's inter-subject FC correlation with every other subject (Airan et al., 2016; Finn and Shen et al., 2015). Using large samples from different publicly available databases, both studies demonstrated the important finding that group-level variability contains differences that are unique and reliable at the individual subject level. Further, they showed that the majority of FC edges that contributed to the successful identification of individuals from within a group were located in heteromodal cortex including the frontoparietal, default, and attentional networks.

1.2. Collection states and FC variability

The effects of acquisition conditions on FC continue to be examined and debated (Arbabshirani et al., 2013; Cole et al., 2014; Mennes et al., 2013). The question in the current context is whether inter-individual differences in FC are more robust under less constrained states such as rest versus tasks. Shah and colleagues showed that individual patterns in FC were preserved across multiple task and rest conditions (Shah et al., 2016). Finn, Shen and colleagues showed that when using an FC-based identification (i.e., matching) algorithm, the maximal accuracy (94%) was attained when using rest-rest correlations; accuracy decreased to 54–87% when using rest-task or task-task correlations, suggesting that individual differences are more easily identified during less constrained states, but are still present in task-based FC data. These studies indicate that inter-individual differences in FC are not abolished when using tasks, at least when the tasks are conventional and discrete such as were used in these studies.

Though the number of studies is currently limited, different results have been demonstrated using more complex, naturalistic tasks. For example, Geerligs and colleagues investigated inter-individual variance during movie watching using a Hitchcock film (*Bang! You're Dead*) (2013). This study showed that the least amount of overlap and the highest amount of FC variance occurred within the movie-task comparison relative to both the movie-rest and task-rest comparisons, suggesting that perhaps movies have a unique effect on FC patterns. To date, it remains unclear which collection states might be most advantageous for the study of FC patterns that are distinct at the individual level.

1.3. Movies and FC variability

Due to the significant improvement in compliance regarding head movement and arousal levels conferred by movie watching in the scanner (Vanderwal et al., 2015), we wanted to evaluate the effects of movie watching on BOLD-signal based FC variability. The present study used two distinct movie-watching conditions (one complex social movie and our low-processing abstract movie) and eyes-open rest. Sequence parameters were kept constant across conditions, and rigorous motion thresholds and correction procedures were used. The study is divided into two parts. First, we characterize multiple aspects of FC variability, including analyses of variance across collection states, measures of within- and between-subject correlations of FC, and the spatial distribution of inter-individual variability of FC. Based on these cross-condition comparisons of variability, we predicted that movies would enhance the ability to detect individual differences in FC that are unique at the individual level. The second part of the study tested this hypothesis. We ran an unsupervised test-retest matching algorithm that used FC matrices to identify individual subjects from among a group. We also ran the algorithm using different parcellation resolutions, acquisition durations, and percentages of edges used to test whether these factors differentially affected the two types of movies and rest. The primary outcome was the accuracy of the identification algorithm across the three conditions. As such, this study is the first to show the spatial distribution of inter-individual variability under naturalistic viewing conditions and to report accuracies of an FC-based identification algorithm using movies.

2. Materials and methods

2.1. Data collection

Participants. Healthy right-handed adults were recruited from the community. Exclusion criteria included neurological or psychiatric diagnoses, use of centrally acting medications, heavy alcohol use, illicit drug use in the past 6 months, cardiovascular disease, significant visual or hearing impairment, and self-reporting less than six hours of sleep per night. Forty-six participants completed two testing sessions with a one-week interval, and 12 participants self-reported falling asleep during one or both sessions and were excluded from further analysis. Three additional subjects were excluded for having fewer than 50% volumes remaining after scrubbing procedures (see below), leaving our final cohort at n = 31 (17 females, mean age 24.5 +/− 5.3 years). Data from a subset (n = 22) were published previously (Vanderwal et al., 2015). All participants gave written consent and were compensated for their participation. The study was approved by the Human Investigations Committee at Yale University School of Medicine.

2.1.1. Procedure

Imaging was performed on a Siemens Trio 3-Tesla scanner with a 32-channel head coil. Standard structural images used an MP-RAGE sequence (TR=1900 ms, TE=2.52 ms, TI=900 ms, flip angle=9°) yielding 1 mm^3 voxel size. Functional data were collected using a single shot echo planar imaging sequence (TR=2500 ms, TE=30 ms, flip angle=80°, voxel size=3 mm isotropic) across 38 slices. All participants completed 3 functional scans during which stimuli were presented via E-Prime software, version 2.0 (Psychology Software Tools, Pittsburgh, PA). Images were back-projected onto a screen that participants viewed via a mirror mounted on the head coil. Sound-reducing headphones over protective earplugs enabled participants to hear the soundtracks. Three 7 min and 20 s conditions included *Inscapes*, a nonverbal, nonsocial series of slowly evolving abstract shapes with a piano score (detailed description of this movie is provided in Vanderwal et al., 2015), a clip from the movie *Ocean's Eleven* (Warner Brothers, 2001, directed by Steven Soderbergh) referred to here as Oceans, and Rest (see Fig. 1). Condition order was counter-balanced across participants. Each condition started and ended with 10 s of fixation; the first 10 s were dropped for all analyses. Participants were asked to watch the screen and to stay as still as possible during each condition. Foam wedges were fitted around the participant's head for comfort and to decrease movement. Retest sessions occurred 1 week later at the same time slot whenever possible. Six participants had different time slots for scan 1 and scan 2, but the 1-week interval was maintained.

2.1.2. Data preprocessing

Standard data preprocessing was performed using the Configurable Pipeline for the Analysis of Connectomes (C-PAC) including motion realignment and transformation into Montreal Neurological Institute (MNI) space using Advanced Normalization Tools (ANTS) (Avants et al., 2008). ANTS employs a series of sequential transformations to optimize image registration, beginning with a rigid and affine linear transformation and ending with a nonlinear diffeomorphic transform (Symmetrical Normalization or SyN) that maximizes the cross-correla-

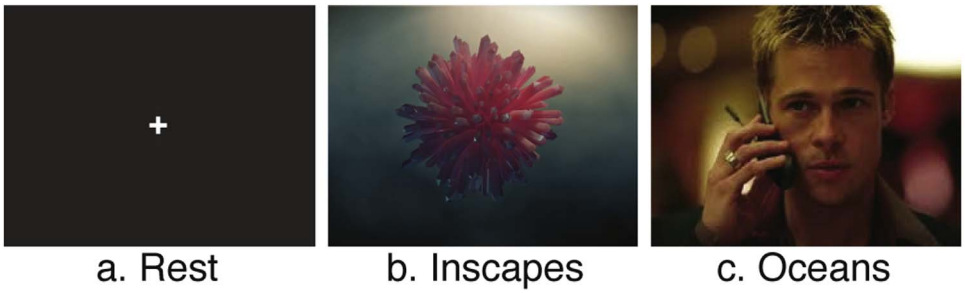

Fig. 1. Three 7-min conditions. Conditions were a) eyes-open Rest with a static fixation cross; b) Inscapes, a nonverbal, nonsocial, abstract animation designed to maintain engagement while minimizing cognitive load; and c) a complex verbal and social clip from the vault scene of the action movie *Ocean's Eleven*. *Inscapes* can be viewed and downloaded at headspacestudios.org.

tion within a map. Nuisance signal regression removed linear and quadratic trends, motion estimates, and COMPCOR with 5 principal components (Behzadi et al., 2007), and was followed by temporal filtering (0.008–0.1 Hz). Motion was evaluated using framewise displacement (FD) which quantifies head motion between each volume of functional data (Power et al., 2012), and volume censoring was used to mitigate motion artifact with a threshold of 0.2 mm, also removing the preceding and 2 subsequent volumes (Power et al., 2014, 2015; Yan et al., 2013). Participants were excluded if they had fewer than 50% (or 86) volumes remaining after scrubbing. Following Finn et al., data were not spatially smoothed prior to averaging within our cluster-based regions of interest (ROIs)(Finn and Shen et al., 2015).

2.1.3. Whole-brain FC matrices

All subsequent analyses were based on FC connectivity matrices. Matrices were constructed using a functional parcellation scheme comprising 200 ROIs (Craddock et al., 2012). For each subject, we extracted the mean time series of each ROI and then computed the Pearson's correlation coefficient between all ROI pairs to produce a 200×200 whole-brain connectivity matrix for each subject for each condition. Subsequent analyses used only unique ROI pairs (i.e., A-B and not B-A), leaving 19 900 edges. Correlation coefficients were Fisher z-transformed, averaged across subjects, and then reverted to r-values to produce group-level correlation matrices. To qualitatively assess similarities across conditions in terms of the correlations within and between large-scale functional networks, we arranged the ROIs on the matrix according to network membership using the 7-network scheme (visual, somatomotor, dorsal attention, ventral attention, limbic, frontoparietal, and default networks; see Fig. 2), defined by Yeo, Krienen, and colleagues (2011).

2.2. FC variance across conditions

Following previous methods used to assess similarity and difference in FC matrices across conditions or states (Cole et al., 2014; Geerligs et al., 2015), we created connectivity matrices for each condition by averaging the connectivity matrices across participants within each condition. These matrices are used to visualize the group-level connectivity for movies and Rest. For statistical comparison across conditions, however, we calculated pairwise Pearson's correlations between connectivity matrices of the different conditions (i.e. Rest-Inscapes, Inscapes-Oceans, Oceans-Rest) within a subject. To better match the noise estimate (see below), we used half the volumes by computing the Pearson's correlation coefficient between the first half of condition 1 and the first half of condition 2, as well as the second half of condition 1 and condition 2. The average of these two correlation coefficients was squared, and this squared value represents the proportion of variance that is shared between those conditions. The remaining variance represents that proportion which differs across states, such that:

- r = correlation between two conditions.
- r^2 = percent shared variance between those conditions, termed overlap.
- $(1 - r^2)$ = total remaining variance, assumed to include both state-based and noise-based contributions.

To estimate the noise contribution to this between-state variance, we calculated the split-half correlation within each condition. The split-half correlation obtained for Rest was used as an estimate of noise regardless of the pair of conditions being compared, as movies are not expected to be consistent from the first half to the second half.

- r_{sh} = split-half correlation of Rest.
- $(1 - r_{sh}^2)$ = estimate of percent variance due to noise.

This facilitates the subtraction of noise from the total variance, such that:

- $(1 - r^2) - (1 - r_{sh}^2)$ = state-based variance.

It is important to note two differences between our method and that outlined in Geerligs et al. (2015). First, all computations were performed using pairwise correlations between connectivity matrices of the different conditions *within* a subject, so we expect lower cross-condition correlations overall. Second, as explained above, the between-condition correlation coefficients are based on only half of the volumes, again likely returning lower r-values than has been shown previously.

2.2.1. Within- and between-subject FC correlations

Within-subject correlations of FC were computed by first calculating the Pearson's correlation coefficient of the two scanning sessions' FC matrices for each subject. To compute the between-subject correlations, we performed the same procedure between one subject and every other subject within a single scanning session. The pairwise correlations were Fisher's z-transformed, averaged, and reverted to r-values to provide a single between- and within-subject value for each subject. As such, these are second-order analyses based on previously calculated cluster-based measures of functional connectivity (i.e., the FC matrices) and are different from first-order analyses of inter-subject functional correlations as performed by Simony et al. (2016).[1] Due to the inherent relatedness among these correlations, particularly the non-independence of the between-subject analysis, we used nonparametric permutation testing (run 10 000 times) to examine the

[1] Inter-subject functional correlations as defined by Simony et al. characterize correlations between the full duration BOLD-signal time-course of seed region 1 in subject A and the time-courses of all regions in subject B, subject C and so forth (2016). This elegant hybrid approach between intersubject correlations and seed-based FC analyses can reveal complex inter-regional patterns of correlations that are stimulus-evoked.

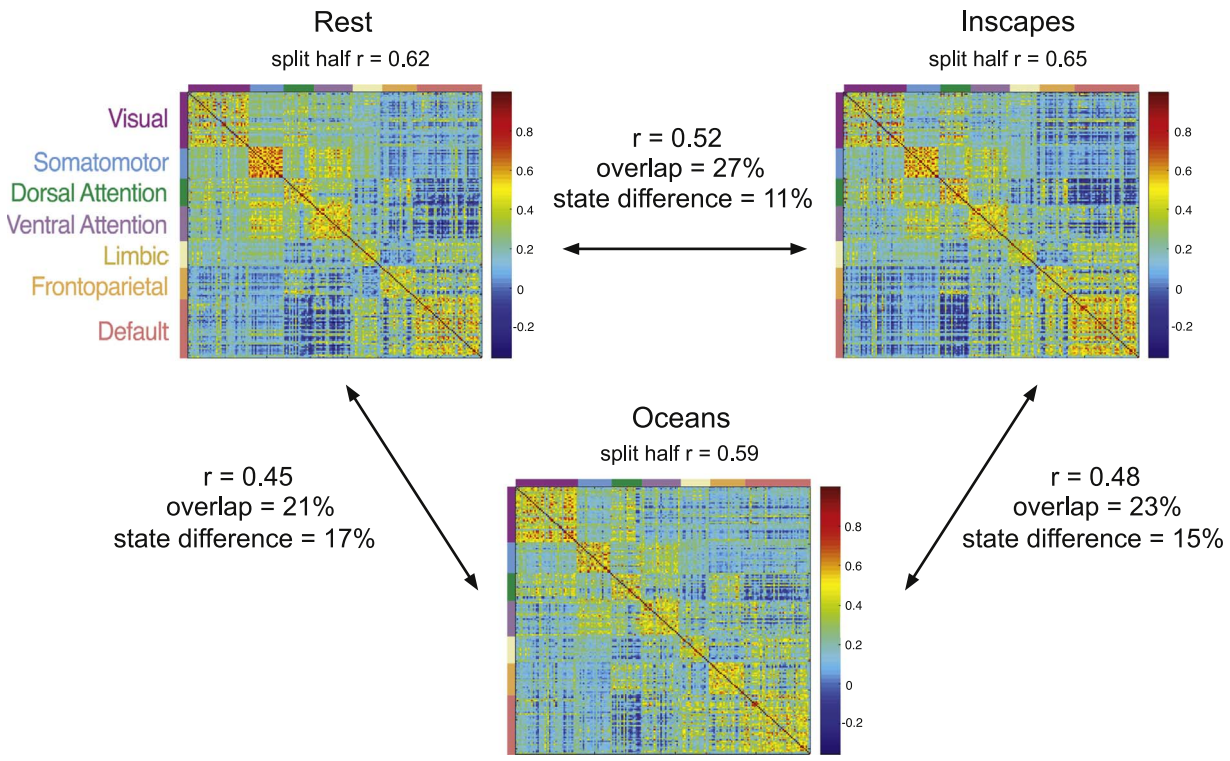

Fig. 2. Similarity and variance in FC matrices across movies and Rest (n=31, healthy adults). Pearson's correlation coefficients were calculated between each pair of conditions to produce the r-value denoted in the matrices. Amongst these moderate correlations, Rest and Inscapes are the most strongly correlated conditions with the highest amount of overlap and the lowest state difference. The split-half correlation for Inscapes was significantly stronger than either Rest or Oceans. These data align with our previous report suggesting Inscapes is associated with FC patterns that more closely resemble Rest than those of conventional movies (Vanderwal et al., 2015).

distribution (Chen et al., 2016).

2.2.2. Spatial distribution of residual inter-individual variability

Following an approach outlined by Mueller et al., we wanted to map cluster-level inter-individual variability of FC using a method that accounted for intra-individual variability (2013). First, group-level total inter-individual variability values were obtained as follows: for each condition's first scanning session we computed a correlation coefficient for each ROI (across all 199 of its edges) between all possible subject pairings. The resulting r-values were subtracted from 1 to convert them to measures of dissimilar variability. Averaging across subject pairs then yielded an estimate of total inter-individual variability at each cluster. Next we computed the intra-individual variability for each condition by performing the same procedure, this time correlating between each subject's scan 1 and scan 2 FC matrices, yielding a 200 × 31 (clusters x subjects) matrix, which was subsequently averaged across individuals to obtain a group-level map. Using ordinary least-squares regression, the intra-individual variability was regressed out of the total inter-individual variability, and the residuals were taken to represent the residual inter-individual variability. We did not regress out a measure of technical noise. Residual values were mapped onto surface space using CARET (Van Essen et al., 2001). To assess the variability by network, we used the 7-network schema from Yeo, Krienen and colleagues, averaging the variability across all clusters belonging to each network (2011). Each cluster was assigned to the network in which the greatest number of its voxels were present. For example, if a cluster had 300 voxels in Network 1 and 100 voxels in Network 2, it was assigned to Network 1.

To test whether regional differences in alignment accuracy might influence measures of variability, we ran a Searchlight algorithm modeled closely after the approach described by Kriegeskorte and colleagues (Kriegeskorte et al., 2006). Spheres (r=15 voxels for anatomical, and r=5 voxels for functional images) were centered around each voxel in the brain and Pearson's correlation coefficients were calculated across the intensity values of each voxel within each sphere between subject A at scan 1, subject A at scan 2, and so on for every subject. The r-value obtained for each sphere was transformed to a measure of variability via subtraction from 1 and assigned to the center voxel. These 1-r values were averaged within clusters and across subjects, and surface projected using CARET. For variability in inter-individual alignment, the same procedure was performed calculating r-values of spheres placed in subject A's anatomical scan at scanning session 1 to the corresponding sphere in the MNI brain. Pearson's correlation coefficients were then calculated between the cluster-based measures of alignment accuracy and cluster-based measures of inter-individual variability to assess if alignment was related to our variability measure.

2.3. Accuracies of identification algorithm

The prediction procedure closely followed methods described elsewhere (Finn and Shen et al., 2015). In brief, six databases were created, one for each of the three conditions for both Scans 1 and 2. Each database consisted of the Crad-200 FC matrix for each subject for a given condition (31 matrices per data set). To run the matching algorithm, two databases were selected at a time. A subject's FC matrix was selected from one, and the Pearson's correlation coefficient was then calculated between that matrix and every matrix in the other database. The two matrices with the highest correlation were deemed the “matched pair," and the accuracy of the algorithm was simply the percentage of correct pairs when checked against the known subject identities. We ran the algorithm across testing sessions and across conditions, resulting in 30 pairings (e.g., Rest 2-Rest 1, Oceans 2-Rest 2, Oceans 2-Rest 1). Because of our moderate sample size, we wanted to be sure that accuracies did not reflect chance pairings. We thus performed nonparametric permutation testing in which false identity pairs were randomly assigned and the algorithm was run 1000 times to determine how many times the false pair was identified as being the

most strongly correlated. To investigate the role of head motion in the matching, we computed discrete motion distribution vectors for each participant based on the framewise displacement time courses across all 3 conditions and across both scanning sessions. The mean and standard deviations of the FD across all subjects and conditions was computed, and 60 bins were set to capture the grand mean +/− 3 standard deviations, and vectors were calculated accordingly. The 1×60 vectors were then used in the same way that the FC matrices were to run the identification algorithm. This procedure tests whether each individual's motion characteristics can be used to identify individuals from within a group, and helps to assess the degree to which motion might contribute to the FC-based matching algorithm. To examine the spatial distribution of the edges that contributed most to successful identification for each condition, we calculated the differential power (DP) for each edge (Finn and Shen et al., 2015). DP indicates the proportion of the time a subject is matched to itself rather than to another subject based on that edge. We then extracted the top 5% of the DP values throughout the brain, and calculated the percentage of edges within each network that met that threshold.

2.3.1. Parcellation resolution

To test if the resolution of the parcellation had a differential effect on identification accuracy across conditions, we parcellated the data at all of the 43 resolutions defined in a publicly available atlas that used a spatially constrained spectral clustering approach of independent resting state data (Craddock et al., 2012). The range of the number of clusters was 10–950. We then ran the identification algorithm using each parcellation on the Scan 2-Scan 1 within-condition pairings. All subsequent analyses used the Crad-200 parcellation and only the Scan 2-Scan 1 within-condition pairings.

2.3.2. Scan duration

To test if shorter scan durations affected the identification accuracy of one condition more than another, we ran the same matching algorithm, varying the amount of data used between two volumes and the full 172 vol run (unscrubbed data were used only for this analysis), starting from the beginning of the run and adding sequential TRs one at a time.

2.3.3. Number of edges

To test if one of the conditions required fewer edges in order to make the correct identity matches, we sequentially tested the algorithm using increasing numbers of edges. To dictate the order in which we added edges, we rank-ordered the edges from least contributory (lowest DP) to most contributory (highest DP) within each condition. Next, we ran the matching algorithm using only the lowest 0.5% of edges, and successively repeated this procedure adding an additional 0.5% at each increment until 100% of the edges were used.

3. Results

3.1. Compliance

Twelve excluded subjects self-reported falling asleep during 14 Rest runs, 7 Inscapes runs, and zero Oceans runs. Head motion at the first scanning session was significantly lower for Inscapes relative to both Rest and Oceans (one-way repeated measures ANOVA, $F_{(2,30)}=4.899$, $p < 0.0001$, post hoc two-tailed *t*-test, Inscapes-Rest p=0.0003, Inscapes-Oceans p=0.01, Oceans-Rest p=0.1). At the second scanning session, no significant differences in head motion were found (one-way repeated measures ANOVA, $F_{(2,30)}=1.32$, p=0.27). See Supplementary Fig 1 for the spread of the FD data. After volume-censoring, the following mean number of volumes remained: Rest 1=152, Inscapes 1=164, Oceans 1=160, Rest 2=155, Inscapes 2=153, and Oceans 2=159.

3.2. FC variance across conditions

Within-condition split-half correlations for FC matrices were as follows: Rest=0.62, Inscapes=0.65, Oceans=0.59 (see Fig. 2). There was a significant effect of condition on split-half correlation (one-way repeated measures ANOVA, $F_{(2,30)}=5.844$, p=0.0048). Follow-up paired *t*-tests showed no significant difference in the split-half correlations between Rest and Inscapes ($t_{(30)}=1.911$, p=0.66) or between Rest and Oceans ($t_{(30)}=1.502$, p=0.1435), with the significant difference found between the split-halves of the two movie conditions ($t_{(30)}=3.404$, p=0.0019). Cross-condition comparisons using half of the volumes showed moderate correlations with significant differences across all comparisons, with Rest-Inscapes r=0.52, Inscapes-Oceans r=0.48 and Oceans-Rest r=0.45 (one-way repeated measures ANOVA, $F_{(2,30)}=20.88$, $p < 0.0001$, post hoc two-tailed *t*-test, Inscapes-Rest vs. Inscapes-Oceans p=0.0013, Rest-Inscapes vs. Rest-Oceans $p < 0.0001$, and Oceans-Rest vs. Oceans-Inscapes p=0.0043). These r-values are lower than those reported by Geerligs et al., possibly because we maintained within-subject pairings and used only half of the volumes when calculating the cross-condition correlations. Rest and Inscapes had the highest overlap at 27% and the lowest state-based difference (after subtracting out a noise estimate) of 11%.

3.3. Within- and between-subject FC correlations

For within-subject correlations, movies were stronger than Rest, but were not different from each other (nonparametric permutation testing Inscapes-Rest p=0.0119, Oceans-Rest p=0.0018, Oceans-Inscapes p=0.5851). For between-subject correlations, movies were again stronger than Rest, and were again not significantly different from each other (nonparametric permutation testing Inscapes-Rest p=0.0008, Oceans-Rest $p < 0.0001$, Oceans-Inscapes p=0.4147, see Fig. 3).

3.4. Spatial distribution of FC variability

Residual inter-individual FC variability (by cluster) demonstrated a nonuniform spatial distribution with higher variability in the lateral prefrontal lobes, temporoparietal junctions, and along regions of the lateral temporal lobes (see Fig. 4). Lower variability was found in primary sensory and motor cortices. This pattern aligns with previous reports (Mueller et al.) and was similar across both movies and Rest. Inscapes had higher variability in temporal regions, while Oceans had higher variability in prefrontal regions. When calculated for each of 7 networks, FC variability was highest in the frontoparietal network and lowest in the visual and somatomotor networks across conditions. Within the frontoparietal network, variability was highest for Oceans. The Searchlight algorithm we ran to examine the spatial distribution of both inter- and intra-subject variability in alignment accuracy showed that alignment overall had strong correlations and low variability, explaining a maximum of 4% of the variance in Fig. 4. Qualitatively, the alignment variability maps did not resemble the inter-individual variability maps, and in particular, the frontoparietal cortex was aligned well (i.e. with low variability) both within and between subjects (See Supplementary Fig 2 for results of the Searchlight analyses). We conclude that the overall spatial pattern of inter-individual variability in FC is not driven by underlying spatial differences in alignment accuracy at either the inter- or intra-individual level.

3.5. Accuracies of identification algorithm

We first tested prediction accuracy using the Crad-200 parcellation, and found high accuracies across and within conditions with a range of 61–100% (see Fig. 5). Oceans attained 100% accuracy, and in general, the highest accuracies were associated with pairings that included movies. Importantly, high accuracies were attained for cross-condition pairings,

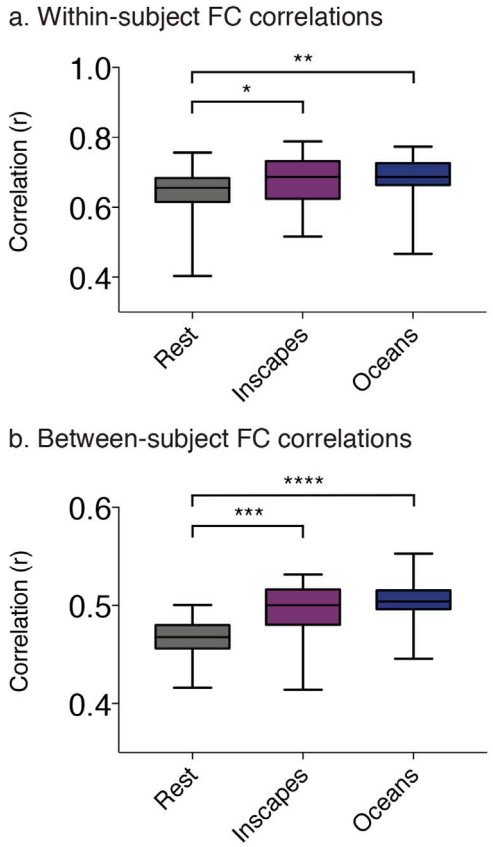

Fig. 3. Within- and between-subject FC correlations. Both movies had significantly greater within-subject correlations relative to Rest, with no significant difference between movies. The same pattern was found for between-subject correlations, with movies greater than Rest (*=p < 0.05, **=p < 0.01, ***=p < 0.001, ****=p < 0.0001, via permutation testing).

indicating that individually distinct patterns in FC persisted across conditions. The permutation testing (performed 1000 times to quantify the percentage of time the algorithm matched a randomly assigned "false identity" pairing) had a mean accuracy of 0.44% (with maximal accuracy of 9.7%) for Scan 2 to Scan 1 pairings, and 0.68% (with maximal accuracy of 6.7%) for Scan 1 to Scan 2 pairings. When using motion distribution to match subjects, accuracies ranged from 0% to 19%. Results for permutation testing and motion distribution are shown in Supplementary Materials. When assessing the network distribution of the top 5% of contributory edges, we found that across conditions, the highest proportion of these edges was found in the frontoparietal network, followed by the ventral and dorsal attention networks.

We also performed a post-hoc analysis in which we ran the identification algorithm again using BOLD-signal time courses instead of FC. The time-course based algorithm yielded accuracies of 0–58% (Supplementary Fig 4). Notably, all pairings using Inscapes and Rest yielded accuracies of 23% or lower, and Oceans-Oceans pairings attained 58%. These data indicate that FC patterns (as opposed to first-order BOLD-signal time courses themselves) drive the high percentages attained in the FC-based algorithm shown in Fig. 5, particularly for Inscapes and Rest.

3.5.1. Parcellation resolution

When tested at different parcellation resolutions, the within-condition Scan 2-Scan 1 identification accuracies improved with higher resolutions, as expected (Fig. 6a). Varying the resolution had differential effects by condition: Oceans attained 100% accuracy at 120 clusters, Inscapes at 500 clusters, and Rest hit a ceiling accuracy of 97% at 550 clusters. Above 600 clusters, cross-condition differences in matching accuracy appear to collapse.

3.5.2. Scan duration

Also as expected, longer scan durations positively affected the accuracy of the algorithm. Oceans reached 100% accuracy at 109 volumes, Inscapes reached maximal accuracy of 97% at 115 volumes, and Rest reached a ceiling accuracy of 90% at 165 volumes (Fig. 6b).

3.5.3. Number of edges used

Again, including higher numbers of edges produced higher prediction accuracies across all conditions, as was expected. Overall, movies had higher accuracies than Rest at all numbers of edges included (Fig. 6c).

4. Discussion

4.1. Accuracies of identification algorithm for movies and rest

This study investigated the effects of movie watching on individual differences in FC. We showed that an unsupervised, FC-based test-retest matching algorithm that identifies subjects from within a group performed well using data acquired during both movies and Rest, and that the highest accuracies were attained using movies.

Overall accuracies of the matching algorithm ranged from 61% to 100%. These results are in-line with data from Finn, Shen and colleagues who reported accuracies of 54–94% in a larger sample using rest and task (Finn and Shen et al., 2015). The highest accuracy in our data (100%) was attained when matching FC matrices between scan sessions of Oceans, with Inscapes reaching 97%, and Rest 90%. The pattern of these accuracy relationships (Oceans > Inscapes > Rest) held true across varying scan durations and number of edges used. We conclude that relative to task-free resting state conditions, movie watching preserves—and possibly enhances—the ability to detect differences in FC patterns that are distinct at the individual level.

4.2. Variability in FC of different acquisition conditions

The matching algorithm used is based on correlations of FC matrices between separate scanning sessions. Consequently, we would expect within-subject correlations to play a substantial role in the success of the algorithm. When examining cluster-wise, whole-brain FC, our data showed that movies had significantly stronger within- and between-subject correlations relative to Rest.

Further, previous work has shown that FC edges which contributed most to successful identification matches were found in the frontoparietal network (Finn and Shen et al., 2015). In our data, variability within the frontoparietal network was greatest for Oceans, perhaps contributing to the observed 100% accuracy attained for the Oceans-Oceans pairings. In general, the spatial distribution of inter-individual variability in FC during Rest and movies followed the same pattern as had been previously reported during Rest: the lowest variability occurred in primary motor and sensory cortices with higher variability in heteromodal cortex involving the prefrontal and temporal cortices (Chen et al., 2015; Mueller et al., 2013). These data suggest that the spatial distribution of residual inter-individual variability observed during Rest is not drastically shifted by movie watching, and more specifically, that variability in the frontoparietal network is high across conditions.

4.3. Individually distinct FC and naturalistic paradigms

To date, the majority of studies utilizing naturalistic paradigms have focused on the concerted nature of BOLD-signal changes evoked by movie watching that have been shown to involve large areas of the cortex (Hasson et al., 2004, 2010; Kauppi et al., 2010). Intuitively, one might assume that because of this shared activation across subjects, patterns of FC would be less distinctive at the individual level. Our data indicate that this is not the case as the highest accuracies of the matching algorithm were attained using movie-watching data. In

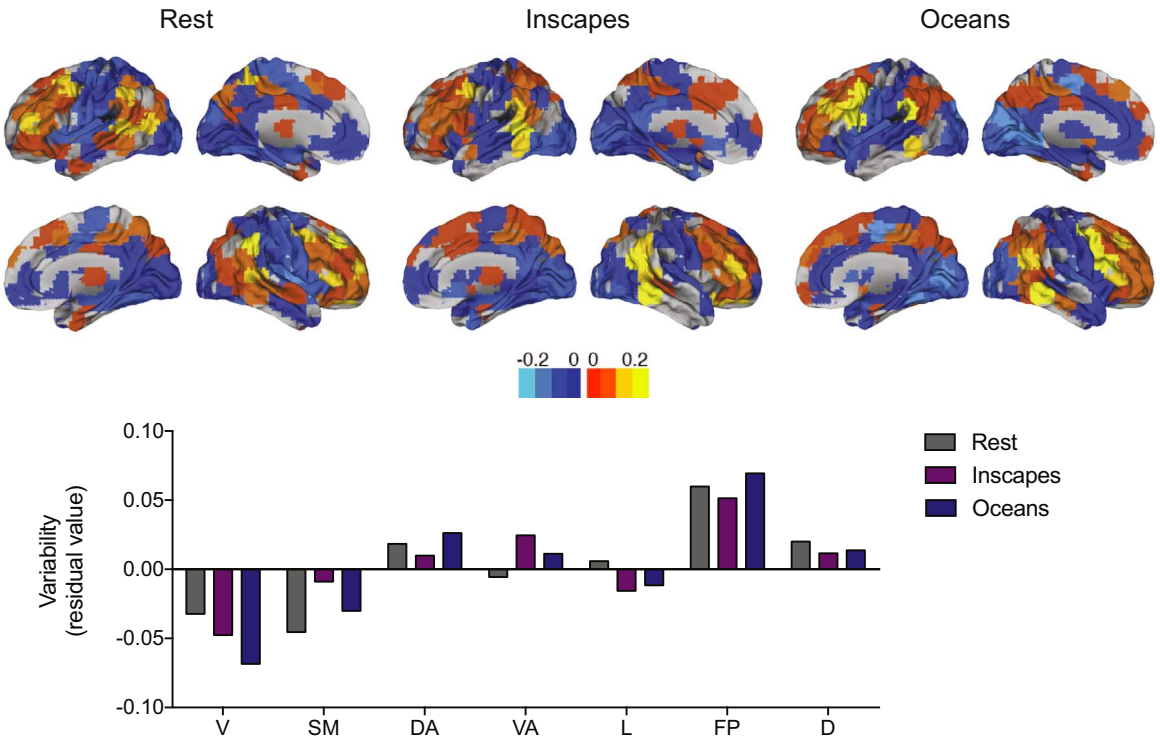

Fig. 4. Spatial distribution of inter-individual variability in FC (n=31, healthy adults). Inter-individual variability was quantified for FC of each cluster after least-squares regression to correct for underlying intra-individual variability. The results of this regression are depicted centered around zero so that warm colors indicate that inter-individual variability is greater than intra-individual variability, and cool colors indicate that intra-individual variability is greater than inter-individual variability. Consistent with previous work (Mueller et al., 2013), FC variability is lowest in primary sensory and motor regions, and highest in heteromodal regions such as lateral prefrontal cortices and the temporoparietal junctions. Qualitatively, this pattern of spatial distribution occurs across all three scanning conditions. Variability by network was highest in the frontoparietal network and lowest in visual and somatomotor networks. V=visual, SM=somatomotor, DA=dorsal attention, VA=ventral attention, L=limbic, FP=frontoparietal, D=default, based on Yeo, Krienen et al. (2011).

addition to the high within-subject FC correlations discussed above, another possible contributing factor to this pattern is that concerted activity across subjects in multiple voxels enables individually distinct patterns of FC to “stand out" more. In other words, we hypothesize that movie watching may not itself evoke individual differences in functional neural responses, but that the whole-brain processing that occurs during naturalistic paradigms across subjects enhances the detection of individually distinct FC patterns. This seems plausible given the fact that cross-condition pairings in our data also attained high accuracies, indicating that the same individually distinct patterns are maintained across conditions.

Relatedly, Papageorgiou et al. suggested that complex stimuli might elicit useful shifts in whole-brain signal-to-noise ratios when they used a highly engaging task in which subjects received real-time feedback to their neural responses during a silent counting task (Papageorgiou et al., 2013). They posited that frontoparietal regions and the insula regulated global processes during engaging conditions, conferring an improvement in signal-to-noise ratios. When taken together with data indicating that individual variability is highest in frontoparietal networks (Mueller et al., 2013), and that matching algorithms rely heavily on edges contained in the frontoparietal network (Finn and Shen et al., 2015), we suggest that during naturalistic conditions, the frontoparietal network may play a dual role in the identification of individually distinct FC patterns. First, frontoparietal FC itself may comprise individually distinct differences in functional connectivity and/or functional mapping, and second, frontoparietal control may cause an advantageous shift in broader processes enhancing the detection of individually distinct FC patterns. Whatever the mechanism, studies to date, including the data presented here, indicate that the frontoparietal network plays a key role in the detection of individual differences in FC.

4.4. Compliance

The major compliance advantage of using movies in healthy adult populations relates to arousal levels. In this study, subjects self-reported falling asleep during 14 Rest runs, 7 Inscapes runs, and zero runs of Oceans. Head movement at the first scan was significantly better during Inscapes relative to both Oceans and Rest. However, no differences in head movement were found at the second session. We speculate that habituation and loss of novelty may have contributed to this null finding.

Because head motion has previously been shown to be more trait-like than state-like (Couvy-Duchesne et al., 2014; Siegel et al., 2016), we were concerned that head motion might contribute to the accuracy of the matching algorithm. When using motion distribution as the basis for an identity algorithm (i.e., with no FC measures), accuracies ranged from 0% to 19%, which is higher than chance but much lower than the accuracies attained using FC measures (61–100%). We conclude that motion likely contributes to the matching of FC matrices, but that it does not account for the primary finding that naturalistic conditions enable the detection of FC differences at the individual level.

4.5. Limitations and future directions

This study has a number of important limitations. The sample size was 31, and because of how the test-retest matching algorithm works, accuracies likely vary critically based on sample size. Future work replicating the movie watching findings in a larger cohort is indicated. The study design also did not include a rich phenotypic assessment, and consequently, we were not able to test for correlations between FC variability during movie watching and clinically relevant behaviors or traits. Because movies appear to enhance the ability to detect individual differences in FC, some brain-behavior relationships may be identified

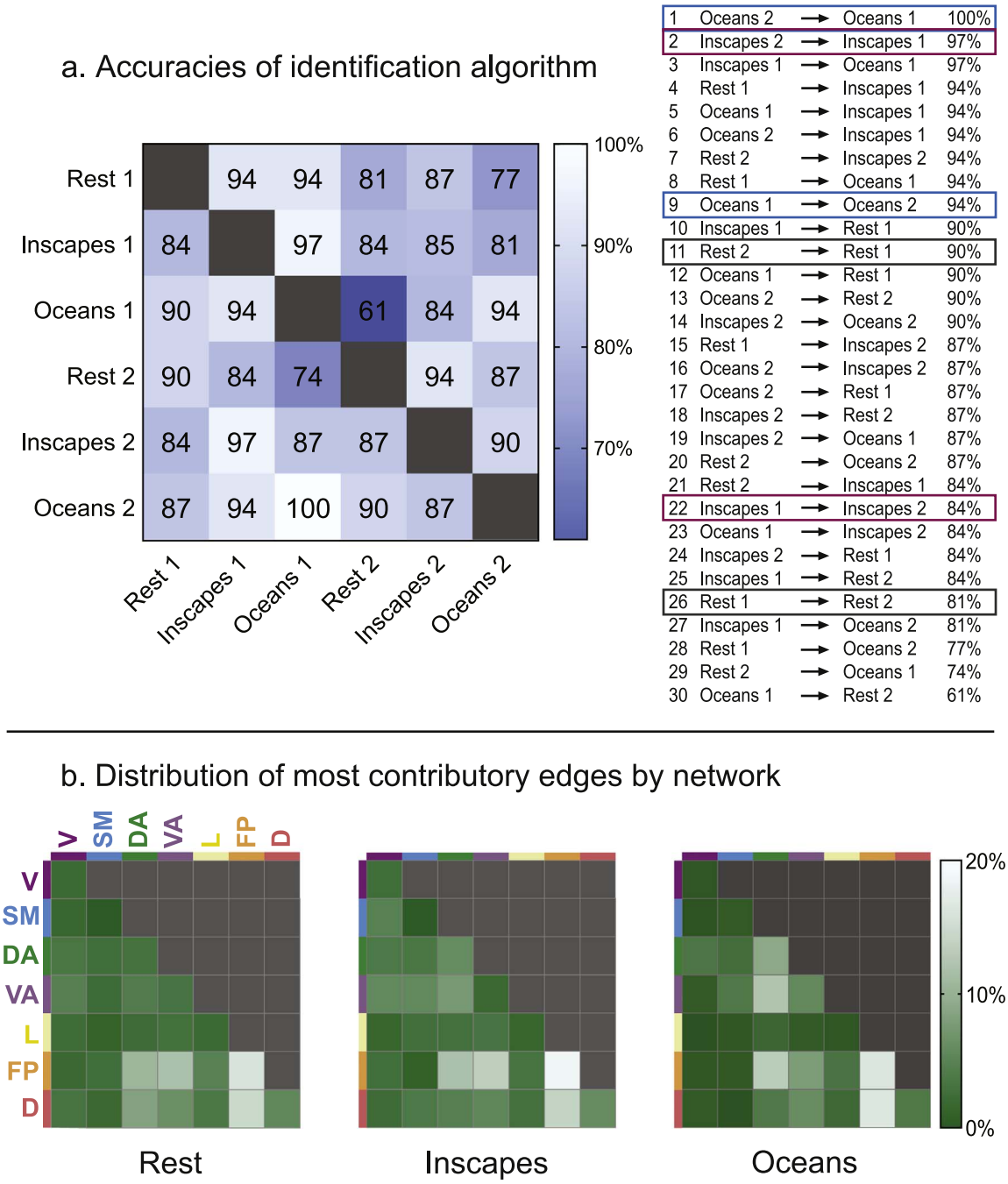

Fig. 5. a. Accuracies of unsupervised test-retest matching algorithm based on FC matrices (n=31, healthy adults). Individual subjects were correctly identified by the unsupervised algorithm across all conditions, with accuracies ranging from 61% to 100%. Overall, the highest accuracies were associated with pairings that involved movies. High accuracies were attained in cross-condition matches, indicating that individual subjects have distinct FC patterns that persist across conditions. b. For all three conditions, the highest proportion of the top 5% of edges contributing to correct identifications were located in the frontoparietal network, followed by the ventral and dorsal attention networks. V=visual, SM=somatomotor, DA=dorsal attention, VA=ventral attention, L=limbic, FP=frontoparietal, D=default, masks for networks based on Yeo et al. (2011).

using naturalistic paradigms that are not detectable using conventional tasks. For example, a pediatric study was able to identify math-based brain-behavior relationships using fMRI data collected during Sesame Street clips that were not detected using a well-validated conventional fMRI math task (Cantlon and Li, 2013).

Further, because we saw cross-condition differences in the number of participants self-reporting sleep, it is likely that cross-condition differences in drowsiness and arousal were also present in the remaining cohort. A recent paper reported that different arousal levels during movie watching modulated the similarity of FC patterns across subjects (Jang et al., 2017). Consequently, the cross-condition differences in classification may be driven by differences in arousal. Future work using electroencephalography and/or other physiological measures of arousal during movie watching and rest would help address this issue. Similarly, though the head motion in our sample was low and we implemented rigorous volume censoring, since we did not utilize global signal regression, it is still possible that cross-condition differences in residual artifact contribute to the classification results (Ciric et al., 2017; Geerligs et al., 2017; Power et al., 2017). Cross-condition differences in temporal dynamics such as rates of network switching are also known to exist under different conditions (Chai et al., 2016; Emerson et al., 2015; Simony et al., 2016) and such differences may contribute to our results, or to individual differences in FC themselves (Liao et al., 2017; Xie et al., 2017). Finally, the cross-

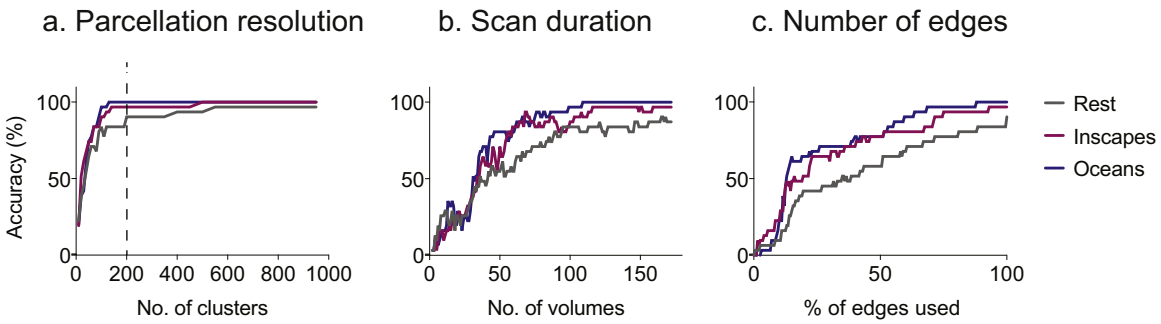

Fig. 6. The effect of varying data parameters on accuracy of unsupervised matching algorithm. a. Parcellation resolution: Using the within-condition matching algorithm (Scan 2-Scan 1) on data parcellated at different resolutions, accuracies increased with higher resolutions. Oceans attained 100% accuracy at 120 clusters, Inscapes at 500 clusters, and Rest hit a ceiling accuracy of 97% at 650 clusters. The dashed line highlights the Crad-200 matrix used for all subsequent analyses. b. Scan duration: Including more volumes led to an increase in accuracy for all conditions. Oceans reached 100% accuracy at 127 volumes; Inscapes reached 97% at 116 volumes; and Rest hit its ceiling of 91% at 165 volumes. c. Number of edges used: After rank-ordering edges according to differential power (DP), we sequentially added edges that were increasingly contributory to successful matching. The more edges used, the higher the accuracy across conditions. Both movies had similar accuracies until about 75% of the edges were used, at which point Oceans diverged from Inscapes. Overall, varying each of these parameters did not alter the general pattern of movies outperforming Rest with regards to the matching of individual subjects. The potential exception to this would be parcellation resolution, where above 600 clusters, cross-condition differences in matching accuracies appear to collapse.

condition accuracy results likely contain individual differences in anatomy and/or functional mapping (Brett et al., 2002; Frost and Goebel, 2012; Shah et al., 2016; Zilles and Amunts, 2013). This interpretation makes sense particularly when looking at the similarity of accuracies across conditions that occurs at higher parcellation resolutions (Fig. 6a). Future studies that incorporate multi-modal or group-weighted parcellation schema (Glasser et al., 2016; Mejia et al., 2015) or explorations of FC in non-anatomical space (Guntupalli et al., 2016) might be combined with the use of naturalistic viewing paradigms to further enhance the sensitivity of fcMRI to identify individually distinct patterns of FC.

4.6. Conclusions

1. Movies preserve, and possibly enhance, the ability to detect patterns in FC that are unique at the individual level.
2. Movies had stronger within- and between-subject correlations in FC relative to Rest; inter-individual variability in the frontoparietal network was highest during Oceans. These factors may underlie the observed 100% matching accuracy attained using Oceans.
3. Compliance benefits of using movies with healthy adults center around arousal levels, with half as many subjects self-reporting sleep during Inscapes relative to Rest, and no subjects self-reporting sleep during Oceans. Significant head motion advantages for healthy adults were found, but only at the first exposure to the stimuli.
4. Movies may be advantageous for future efforts to identify brain-behavior correlations in pediatric and psychiatric populations.

Acknowledgements

The authors thank Uri Hasson (Princeton University) and Linda C. Mayes (Yale Child Study Center) for helpful comments during manuscript preparation. Dr. Vanderwal acknowledges the Allison Family Foundation, the American Academy of Child and Adolescent Psychiatry and the Klingenstein Third Generation Foundation for funding support. *Inscapes* is copyright of Yale University, 2013, and can be downloaded at headspacestudios.org or by emailing the corresponding author.

Appendix A. Supporting information

Supplementary data associated with this article can be found in the online version at doi:10.1016/j.neuroimage.2017.06.027.

References

Airan, R.D., Vogelstein, J.T., Pillai, J.J., Caffo, B., Pekar, J.J., Sair, H.I., 2016. Factors affecting characterization and localization of interindividual differences in functional connectivity using MRI. Hum. Brain Mapp. 37, 1986–1997.
Arbabshirani, M.R., Havlicek, M., Kiehl, K.A., Pearlson, G.D., Calhoun, V.D., 2013. Functional network connectivity during rest and task conditions: a comparative study. Hum. Brain Mapp. 34, 2959–2971.
Avants, B.B., Epstein, C.L., Grossman, M., Gee, J.C., 2008. Symmetric diffeomorphic image registration with cross-correlation: evaluating automated labeling of elderly and neurodegenerative brain. Med Image Anal. 12, 26–41.
Behzadi, Y., Restom, K., Liau, J., Liu, T.T., 2007. A component based noise correction method (CompCor) for BOLD and perfusion based fMRI. Neuroimage 37, 90–101.
Brett, M., Johnsrude, I.S., Owen, A.M., 2002. The problem of functional localization in the human brain. Nat. Rev. Neurosci. 3, 243–249.
Cantlon, J.F., Li, R., 2013. Neural activity during natural viewing of Sesame Street statistically predicts test scores in early childhood. PLoS Biol. 11, e1001462.
Chai, L.R., Mattar, M.G., Blank, I.A., Fedorenko, E., Bassett, D.S., 2016. Functional network dynamics of the language system. Cereb. Cortex..
Chen, B., Xu, T., Zhou, C.L., Wang, L.Y., Yang, N., Wang, Z., Dong, H.M., Yang, Z., Zang, Y.F., Zuo, X.N., Weng, X.C., 2015. Individual variability and test-retest reliability revealed by ten repeated resting-state brain scans over one month. Plos One, 10.
Chen, G., Shin, Y.W., Taylor, P.A., Glen, D.R., Reynolds, R.C., Israel, R.B., Cox, R.W., 2016. Untangling the relatedness among correlations, part I: nonparametric approaches to inter-subject correlation analysis at the group level. Neuroimage 142, 248–259.
Ciric, R., Wolf, D.H., Power, J.D., Roalf, D.R., Baum, G.L., Ruparel, K., Shinohara, R.T., Elliott, M.A., Eickhoff, S.B., Davatzikos, C., Gur, R.C., Gur, R.E., Bassett, D.S., Satterthwaite, T.D., 2017. Benchmarking of participant-level confound regression strategies for the control of motion artifact in studies of functional connectivity. Neuroimage.
Cole, M.W., Bassett, D.S., Power, J.D., Braver, T.S., Petersen, S.E., 2014. Intrinsic and task-evoked network architectures of the human brain. Neuron 83, 238–251.
Couvy-Duchesne, B., Blokland, G.A., Hickie, I.B., Thompson, P.M., Martin, N.G., de Zubicaray, G.I., McMahon, K.L., Wright, M.J., 2014. Heritability of head motion during resting state functional MRI in 462 healthy twins. Neuroimage 102 (Pt 2), 424–434.
Craddock, R.C., James, G.A., Holtzheimer, P.E., 3rd, Hu, X.P., Mayberg, H.S., 2012. A whole brain fMRI atlas generated via spatially constrained spectral clustering. Hum. Brain Mapp. 33, 1914–1928.
Damoiseaux, J.S., Rombouts, S.A., Barkhof, F., Scheltens, P., Stam, C.J., Smith, S.M., Beckmann, C.F., 2006. Consistent resting-state networks across healthy subjects. Proc. Natl. Acad. Sci. USA 103, 13848–13853.
Emerson, R.W., Short, S.J., Lin, W., Gilmore, J.H., Gao, W., 2015. Network-level connectivity dynamics of movie watching in 6-year-old children. Front Hum. Neurosci. 9, 631.
Finn, E.S., Shen, X., Scheinost, D., Rosenberg, M.D., Huang, J., Chun, M.M., Papademetris, X., Constable, R.T., 2015. Functional connectome fingerprinting: identifying individuals using patterns of brain connectivity. Nat. Neurosci. 18, 1664–1671.
Frost, M.A., Goebel, R., 2012. Measuring structural-functional correspondence: spatial variability of specialised brain regions after macro-anatomical alignment. Neuroimage 59, 1369–1381.
Geerligs, L., Rubinov, M., Cam, C., Henson, R.N., 2015. State and trait components of functional connectivity: individual differences vary with mental state. J. Neurosci. 35, 13949–13961.
Geerligs, L., Tsvetanov, K.A., Cam, C., Henson, R.N., 2017. Challenges in measuring individual differences in functional connectivity using fMRI: the case of healthy aging. Hum. Brain Mapp..

Glasser, M.F., Coalson, T.S., Robinson, E.C., Hacker, C.D., Harwell, J., Yacoub, E., Ugurbil, K., Andersson, J., Beckmann, C.F., Jenkinson, M., Smith, S.M., Van Essen, D.C., 2016. A multi-modal parcellation of human cerebral cortex. Nature.
Gordon, E.M., Laumann, T.O., Adeyemo, B., Gilmore, A.W., Nelson, S.M., Dosenbach, N.U., Petersen, S.E., 2017. Individual-specific features of brain systems identified with resting state functional correlations. Neuroimage 146, 918–939.
Guntupalli, J.S., Hanke, M., Halchenko, Y.O., Connolly, A.C., Ramadge, P.J., Haxby, J.V., 2016. A model of representational spaces in human cortex. Cereb. Cortex.
Hasson, U., Malach, R., Heeger, D.J., 2010. Reliability of cortical activity during natural stimulation. Trends Cogn. Sci. 14, 40–48.
Hasson, U., Nir, Y., Levy, I., Fuhrmann, G., Malach, R., 2004. Intersubject synchronization of cortical activity during natural vision. Science 303, 1634–1640.
Insel, T., Cuthbert, B., Garvey, M., Heinssen, R., Pine, D.S., Quinn, K., Sanislow, C., Wang, P., 2010. Research domain criteria (RDoC): toward a new classification framework for research on mental disorders. Am. J. Psychiatry 167, 748–751.
Jang, C., Knight, E.Q., Pae, C., Park, B., Yoon, S.A., Park, H.J., 2017. Individuality manifests in the dynamic reconfiguration of large-scale brain networks during movie viewing. Sci. Rep. 7, 41414.
Kauppi, J.P., Jaaskelainen, I.P., Sams, M., Tohka, J., 2010. Inter-subject correlation of brain hemodynamic responses during watching a movie: localization in space and frequency. Front Neuroinform 4, 5.
Kriegeskorte, N., Goebel, R., Bandettini, P., 2006. Information-based functional brain mapping. Proc. Natl. Acad. Sci. USA 103, 3863–3868.
Liao, X., Cao, M., Xia, M., He, Y., 2017. Individual differences and time-varying features of modular brain architecture. Neuroimage 152, 94–107.
Mejia, A.F., Nebel, M.B., Shou, H., Crainiceanu, C.M., Pekar, J.J., Mostofsky, S., Caffo, B., Lindquist, M.A., 2015. Improving reliability of subject-level resting-state fMRI parcellation with shrinkage estimators. Neuroimage 112, 14–29.
Mennes, M., Kelly, C., Colcombe, S., Castellanos, F.X., Milham, M.P., 2013. The extrinsic and intrinsic functional architectures of the human brain are not equivalent. Cereb. Cortex 23, 223–229.
Mueller, S., Wang, D., Fox, M.D., Yeo, B.T., Sepulcre, J., Sabuncu, M.R., Shafee, R., Lu, J., Liu, H., 2013. Individual variability in functional connectivity architecture of the human brain. Neuron 77, 586–595.
O'Connor David, N.V.P., Kovacs, Meagan, Xu, Ting, Ai, Lei, Pellman, John, Vanderwal, Tamara, Parra, Lucas, Cohen, Samantha, Ghosh, Satrajit, Escalera, Jasmine, Grant-Villegas, Natalie, Osman, Yael, Bui, Anastasia, Cameron Craddock, Richard, Peter Milham, Michael, 2016. The healthy brain network serial scanning Initiative: a resource for evaluating inter-individual differences and their reliabilities across scan conditions and sessions. bioRxiv, 078881.
Papageorgiou, T.D., Lisinski, J.M., McHenry, M.A., White, J.P., LaConte, S.M., 2013. Brain-computer interfaces increase whole-brain signal to noise. Proc. Natl. Acad. Sci. USA 110, 13630–13635.
Power, J.D., Barnes, K.A., Snyder, A.Z., Schlaggar, B.L., Petersen, S.E., 2012. Spurious but systematic correlations in functional connectivity MRI networks arise from subject motion. Neuroimage 59, 2142–2154.
Power, J.D., Mitra, A., Laumann, T.O., Snyder, A.Z., Schlaggar, B.L., Petersen, S.E., 2014. Methods to detect, characterize, and remove motion artifact in resting state fMRI. Neuroimage 84, 320–341.
Power, J.D., Plitt, M., Laumann, T.O., Martin, A., 2017. Sources and implications of whole-brain fMRI signals in humans. Neuroimage 146, 609–625.
Power, J.D., Schlaggar, B.L., Petersen, S.E., 2015. Recent progress and outstanding issues in motion correction in resting state fMRI. Neuroimage 105, 536–551.
Rosenberg, M.D., Finn, E.S., Scheinost, D., Papademetris, X., Shen, X., Constable, R.T., Chun, M.M., 2016. A neuromarker of sustained attention from whole-brain functional connectivity. Nat. Neurosci. 19, 165–171.
Shah, L.M., Cramer, J.A., Ferguson, M.A., Birn, R.M., Anderson, J.S., 2016. Reliability and reproducibility of individual differences in functional connectivity acquired during task and resting state. Brain Behav., e00456.
Shehzad, Z., Kelly, A.M., Reiss, P.T., Gee, D.G., Gotimer, K., Uddin, L.Q., Lee, S.H., Margulies, D.S., Roy, A.K., Biswal, B.B., Petkova, E., Castellanos, F.X., Milham, M.P., 2009. The resting brain: unconstrained yet reliable. Cereb. Cortex 19, 2209–2229.
Shen, X., Finn, E.S., Scheinost, D., Rosenberg, M.D., Chun, M.M., Papademetris, X., Constable, R.T., 2017. Using connectome-based predictive modeling to predict individual behavior from brain connectivity. Nat. Protoc. 12, 506–518.
Siegel, J.S., Mitra, A., Laumann, T.O., Seitzman, B.A., Raichle, M., Corbetta, M., Snyder, A.Z., 2016. Data quality influences observed links between functional connectivity and behavior. Cereb. Cortex.
Simony, E., Honey, C.J., Chen, J., Lositsky, O., Yeshurun, Y., Wiesel, A., Hasson, U., 2016. Dynamic reconfiguration of the default mode network during narrative comprehension. Nat. Commun. 7, 12141.
Van Essen, D.C., Drury, H.A., Dickson, J., Harwell, J., Hanlon, D., Anderson, C.H., 2001. An integrated software suite for surface-based analyses of cerebral cortex. J. Am. Med Inform. Assoc. 8, 443–459.
Vanderwal, T., Kelly, C., Eilbott, J., Mayes, L.C., Castellanos, F.X., 2015. Inscapes: a movie paradigm to improve compliance in functional magnetic resonance imaging. Neuroimage 122, 222–232.
Xie, H., Calhoun, V.D., Gonzalez-Castillo, J., Damaraju, E., Miller, R., Bandettini, P.A., Mitra, S., 2017. Whole-brain connectivity dynamics reflect both task-specific and individual-specific modulation: a multitask study. Neuroimage.
Yan, C.G., Cheung, B., Kelly, C., Colcombe, S., Craddock, R.C., Di Martino, A., Li, Q., Zuo, X.N., Castellanos, F.X., Milham, M.P., 2013. A comprehensive assessment of regional variation in the impact of head micromovements on functional connectomics. Neuroimage 76, 183–201.
Yeo, B.T., Krienen, F.M., Sepulcre, J., Sabuncu, M.R., Lashkari, D., Hollinshead, M., Roffman, J.L., Smoller, J.W., Zollei, L., Polimeni, J.R., Fischl, B., Liu, H., Buckner, R.L., 2011. The organization of the human cerebral cortex estimated by intrinsic functional connectivity. J. Neurophysiol. 106, 1125–1165.
Zilles, K., Amunts, K., 2013. Individual variability is not noise. Trends Cogn. Sci. 17, 153–155.
Zuo, X.N., Kelly, C., Adelstein, J.S., Klein, D.F., Castellanos, F.X., Milham, M.P., 2010. Reliable intrinsic connectivity networks: test-retest evaluation using ICA and dual regression approach. Neuroimage 49, 2163–2177.